

RESEARCH

Open Access



# Neuron-restricted cytomegalovirus latency in the central nervous system regulated by CD4<sup>+</sup> T-cells and IFN- $\gamma$

Fran Krstanović<sup>1</sup>, Andrea Mihalić<sup>1</sup>, Ahmad Seyar Rashidi<sup>2</sup>, Katarzyna M. Sitnik<sup>3,5</sup>, Zsolt Ruzsics<sup>4</sup>, Luka Čičin-Šain<sup>5,6</sup>, Georges M. G. M. Verjans<sup>2</sup>, Stipan Jonjić<sup>1,7</sup> and Ilija Brizić<sup>1\*</sup>

## Abstract

All human herpesviruses establish latency following the resolution of the primary infection. Among these,  $\alpha$ -herpesviruses HSV-1, HSV-2 and VZV establish latency in neurons, whereas neurons are not traditionally considered a site of latency for other herpesviruses. Using a combination of in vivo murine models and ex vivo human fetal tissues, we discovered that cytomegalovirus (CMV), a ubiquitous  $\beta$ -herpesvirus, can persist in neurons and that CD4<sup>+</sup> T-cell-derived interferon-gamma is critical in restricting active viral replication in this cell type. Furthermore, we show that mouse CMV can establish latency in neurons and that CD4<sup>+</sup> T-cells are essential in preventing viral reactivation. Our findings may have translational significance because human cytomegalovirus (HCMV) is the leading cause of congenital viral infections resulting in neurodevelopmental and neuroinflammatory lesions with long-term functional sequelae.

**Keywords** Cytomegalovirus, Congenital CMV, Viral latency, Neurons, CD4<sup>+</sup> T-cells, Hippocampus

## Introduction

Human cytomegalovirus (HCMV) is a highly prevalent herpesvirus, with most of the population worldwide being seropositive [1]. Approximately 1% of infants are born with congenital HCMV (cHCMV) infection, making it the most common congenital viral infection [2]. Newborns infected with HCMV can develop severe disease, including neurodevelopmental and neuroinflammatory disorders, leading to functional sequelae such as intellectual disability and sensorineural hearing loss (SNHL) [2]. The mechanisms by which the virus spreads to the brain and induces pathology remain poorly understood, largely due to the reliance on observational and histopathological studies of brain specimens from severe cHCMV cases [3].

Like most human and animal herpesviruses, HCMV exhibits strict species specificity and cannot be used to infect laboratory animals in order to model and

\*Correspondence:

Ilija Brizić  
ilija.brizic@uniri.hr

<sup>1</sup>Center for Proteomics, Faculty of Medicine, University of Rijeka, 51000 Rijeka, Croatia

<sup>2</sup>HerpeslabNL of the Department of Viroscience, Erasmus Medical Center, 3015 GD Rotterdam, The Netherlands

<sup>3</sup>Department of Biological Sciences and Pathobiology, University of Veterinary Medicine Vienna, Vienna 1210, Austria

<sup>4</sup>Institute of Virology, Faculty of Medicine, University Medical Center Freiburg, University of Freiburg, 79104 Freiburg, Germany

<sup>5</sup>Department of Viral Immunology, Helmholtz Centre for Infection Research, 38124 Braunschweig, Germany

<sup>6</sup>Centre for Individualized Infection Medicine, Helmholtz Centre for Infection Research and the Hannover Medical School, 30625 Hannover, Germany

<sup>7</sup>Department of Biomedical Sciences, Croatian Academy of Sciences and Arts, 51000 Rijeka, Croatia



© The Author(s) 2025. **Open Access** This article is licensed under a Creative Commons Attribution-NonCommercial-NoDerivatives 4.0 International License, which permits any non-commercial use, sharing, distribution and reproduction in any medium or format, as long as you give appropriate credit to the original author(s) and the source, provide a link to the Creative Commons licence, and indicate if you modified the licensed material. You do not have permission under this licence to share adapted material derived from this article or parts of it. The images or other third party material in this article are included in the article's Creative Commons licence, unless indicated otherwise in a credit line to the material. If material is not included in the article's Creative Commons licence and your intended use is not permitted by statutory regulation or exceeds the permitted use, you will need to obtain permission directly from the copyright holder. To view a copy of this licence, visit <http://creativecommons.org/licenses/by-nc-nd/4.0/>.

investigate the HCMV disease in non-human species. However, the pathophysiology of the mouse CMV (MCMV) infection closely mimics that of HCMV infections, including spread and virus-induced neuropathology, underlining its value in deciphering the virus-host interactions [4, 5]. To model cHCMV infection, we are infecting newborn mice by the intraperitoneal (i.p.) route within the first postnatal day [5, 6]. Following infection of newborn mice, MCMV disseminates to several organs, including the brain, and initiates a local innate and subsequent adaptive immune response [7, 8]. As in infants with cCMV infection, CMV infection in newborn mice is associated with an inflammation of the CNS, altered brain development, as well as sensorineural hearing loss [4, 6]. Following the resolution of the acute infection, MCMV establishes a latent infection in the brain, reshaping the immune state of this organ as tissue-resident memory T-cells ( $T_{RM}$  cells) are retained in the brain [10]. Notably, the cellular site of CMV latency and the mechanisms by which T-cells control viral infection in the brain are still unknown.

In this study, we aimed to elucidate viral dissemination and tropism in a mouse model of cHCMV infection, as well as the immune mechanisms controlling the infection in brain cells. Using recombinant reporter viruses and transgenic mouse lines, we reveal that MCMV disseminates and productively infects principal central nervous system (CNS) resident cells with different kinetics and has a remarkable propensity for infecting hippocampal cells. We also demonstrate that neurons are the main source of infectious virus during the late phase of acute infection. Finally, we show that IL-12,  $CD4^+$  T-cells, and IFN- $\gamma$  are essential for suppressing viral replication, establishing latency, and preventing reactivation in neurons.

## Materials and methods

### Mice

Mice were strictly age-matched within experiments and handled in accordance with institutional and national guidelines. Newborn mice of both sexes were included in all experiments. All mice were housed and bred under specific pathogen-free conditions at the animal facility of the Faculty of Medicine, University of Rijeka, where they were maintained at 22 °C in a 12-hour light-dark cycle and relative humidity (40–50%). Wild-type C57BL/6J (strain #000664), GFAP-Cre line 77.6 (#024098), Sall1CreERT2 (provided by Ryuchi Nishinakamura at Kumamoto University [11, 12]), BAF53b-Cre (#027826),  $CD4^{-/-}$  (#002663),  $CD8^{-/-}$  (#002665),  $Prf1^{-/-}$  (#002407),  $Gzma^{-/-}Gzmb^{-/-}$  (#010608),  $TNFRp55^{-/-}$  (#002818),  $Ifng^{-/-}$  (#002287), and  $Il12rb2^{-/-}$  (#003248) and Rosa26-loxP-tdTomato (#007914) mice were obtained from The Jackson Laboratory. The Animal

Welfare Committee at the University of Rijeka, Faculty of Medicine, and The National Ethics Committee for the Protection of Animals Used for Scientific Purposes (Ministry of Agriculture) approved all animal experiments (UP/I-322-01/19–01/58, UP/I-322-01/21–01/51, UP/I-322-01/23–01/33).

### Viruses and cell lines

Tissue culture-derived wild-type (WT) MCMV reconstituted from BAC pSM3fr-MCK-2fl was used in the majority of experiments [13]. MCMV- $\Delta m157$ -flox-egfp (MCMV-flox) was previously described [14]. MCMV-GFP\_Cre ( $\Delta IE2$ ) expressing EGFP and Cre recombinase under the control of the endogenous MIEP promoter was generated by replacing the entire IE2 ORF with a construct encoding Cre recombinase in MCMV<sup>IE-GFP</sup> [15], in which a construct encoding EGFP plus a distal P2A-encoding sequence is inserted in the start codon of IE1/3. The backbone of MCMV-GFP\_Cre ( $\Delta IE2$ ) is the Mck2-repaired BAC-encoded MCMV strain, clone pSM3fr-MCK-2-fl 3.3 [13], and genetic modifications were done using *en passant* mutagenesis [16].

Virus stocks and organ homogenates were titrated on mouse embryonic fibroblasts (MEFs) using standard plaque assay procedures [6]. Newborn pups were infected i.p. 24–48 h postnatally with either 200 plaque-forming units (PFU) of WT MCMV, 1500 PFU of recombinant MCMV-flox, or 1000 PFU of recombinant MCMV-GFP\_Cre. Recombinant viruses MCMV-flox and MCMV-GFP\_Cre are attenuated compared to the WT MCMV strains and were thus administered at higher doses in order for the viral load in mice infected with these viruses to reach levels comparable to virus levels in animals infected with the WT MCMV. For HCMV infection experiments RV-TB40-BACKL7-SE-EGFP (KL7-EGFP HCMV) virus was used, a kind gift from Christian Sinzger [17].

SH-SY5Y cells were infected with KL7-EGFP HCMV at a multiplicity of infection (MOI) of 10 diluted in 500  $\mu$ l of culture medium. For treatment experiments, cells were treated with 100, 1000, or 2500 U/ml of recombinant human IFN- $\gamma$  (Peprotech, #300-02) diluted in 500  $\mu$ l of culture medium. The fluorescence intensity pseudocolor images of SH-SY5Y cells were acquired using the Amersham Typhoon Biomolecular Imager (GE Healthcare). Grayscale intensity values in the obtained images, which are proportional to the GFP fluorescence intensity, have then been remapped to the green channel in the 8-bit RGB color space (range 0–255) using the pseudocolor image look-up-tables available in ImageJ v1.54 [18]. The average pixel intensities in the green channel for each well were then determined using the ReadPlate v3.0 ImageJ plugin and used as representatives of average

GFP fluorescence per well (1.54n, National Institutes of Health) [19].

#### Tamoxifen administration

To induce site-specific recombination in CreERT2 transgenic mice, TAM (Sigma-Aldrich, #T5648) was dissolved in corn oil (Sigma-Aldrich, #C8267) to prepare 10 mg/ml stock solutions [20]. On 1–3 days post-infection (dpi), 50 µg of TAM in a volume of 50 µL was administered daily by intragastric (i.g.) injection using a 30G needle (BD Microlance, #304000).

#### Immunohistological procedures

Mouse brains were fixed in 4% paraformaldehyde and paraffin-embedded. Double immunohistochemical staining was performed on mouse brains for the detection of viral antigen and the detection of CNS cell types. Antigen retrieval was performed in a citrate buffer. Endogenous peroxidase activity was blocked with peroxidase and alkaline phosphatase blocking reagent (Dako, #S200380) for 10 min. Nonspecific binding was blocked with 3% BSA (Roth, #8076.1). Viral antigen IE1 was detected using biotinylated (ThermoFisher Scientific, #A39256) anti-IE1 antibody (clone IE1.01; Center for Proteomics, Faculty of Medicine, University of Rijeka, Rijeka, Croatia, #HR-MCMV-12). Antibody binding was visualized with streptavidin alkaline phosphatase conjugate (1:1000, Roche, #11089153001), followed by liquid permanent red as a chromogen (Dako, #K064030). CNS cells were detected with rabbit anti-Iba-1 (1:1000, Fujifilm; Wako Chemicals, #019-19741) for microglia, rabbit anti-GFAP (1:200, Cell signaling, #80788) for astrocytes and rabbit anti-MAP2 (1:1000, Abcam, #ab183830) antibody for neurons. Antibody binding was visualized with peroxidase-conjugated goat anti-rabbit IgG antibody (1:500, Abcam, #ab6721), followed by 3,3'-diaminobenzidine (DAB) as a chromogen (Dako, #GC80611-2). Tissues were counterstained with hematoxylin (Shandon, #12687926). Images were acquired with Olympus BX51, 100x magnification (oil).

For the preparation of frozen brain tissues, mice were first perfused with PBS, and brains were fixed in 4% paraformaldehyde. Following fixation, brains were submerged in 30% sucrose-PBS. The tissue was frozen on dry ice in OCT (Sakura, #4583) embedding media and stored at -80 °C until cutting. Before staining, tissue slides were blocked with 3% BSA. CNS cells were detected with rabbit anti-Iba-1 (1:1000, Fujifilm; Wako Chemicals, #019-19741) for microglia, rabbit anti-GFAP (1:200, Cell signaling, #80788) for astrocytes and rabbit anti-NeuN (1:250, Cell signaling, #12943) for neurons. Primary antibodies were labeled with goat anti-rabbit IgG antibody conjugated to Alexa Fluor (AF) 647 (1:250, Abcam, #ab150083). Nuclei were stained with 4',6-Diamidino-2-Phenylindole (DAPI) (Biolegend, #422801).

#### MCMV reactivation assays

To induce MCMV reactivation *in vivo*, mice were depleted of CD4<sup>+</sup> T-cells by administering 150 µg of anti-CD4 antibody (GK1.5, BioXCell, #BE0003-1) *i.p.* every 4–5 days for 30 days. Brains were collected, and the tissue was homogenized and centrifuged for 1 min at 400 *g*. The supernatant was collected, mixed with 5 ml of 3% DMEM medium, and distributed on a 24-well plate seeded with MEF. Plates were left to incubate for 5–6 days. Afterward, supernatants were transferred to new 24-well plates with MEF and analyzed for plaque formation after 5–6 days of incubation.

*Ex vivo* reactivation was performed using a previously published procedure [21]. Brains were collected, hemispheres were separated sagittally, and cortex, hippocampus and cerebellum were dissected from each hemisphere. Tissues were cultured in 1 ml of 3% DMEM media in individual wells of 24-well plates for 6 weeks. The supernatant was collected weekly, culture media was replaced, and infectious virus was detected by the plaque assay.

#### Flow cytometry and cell sorting

Mice were sacrificed, and brains were collected in RPMI 1640 with 3% FCS and mechanically dissociated. Single-cell suspensions of brains were prepared according to standard protocols (8). In brief, 30% Percoll (Cytiva, #17089101) and brain homogenate suspension was underlaid with 70% Percoll in PBS and then centrifuged at 1,800 rpm for 25 min. Cells in the interphase were collected for further analysis of microglia and T-cell populations. Adult Brain Dissociation Kit (Miltenyi Biotec, #130-107-677) was used to isolate astrocytes, microglia, and oligodendrocytes from the brain. After tissue dissociation based on enzymatic digestion (enzyme papain), debris, and red blood cell removal, myelin was additionally removed using magnetic beads (Myelin Removal Beads, Miltenyi Biotec, #130-096-433). Flow cytometric analysis was performed using following anti-mouse antibodies: CD45.2 (104), CD11b (M1/70), CD8a (53–6.7), CD4 (RM4-5), CD69 (H1.2F3), CD103 (2E7), CD3e (145-2C11), CD19 (eBio1D3), O1 (O1) purchased from ThermoFisher. ACSA-2 antibody (IH3-18A3) was purchased from Miltenyi Biotec. CD31 (MEC13.3), PDGFRα (APA5), Ly6C (HK1.4) and CD29 (HMβ1-1) antibodies were purchased from BioLegend. All data were acquired using a FACSAria (BD Biosciences). Microglia and astrocytes were sorted by FACS. Microglia were sorted as CD45.2<sup>int</sup>CD11b<sup>+</sup> population, while astrocytes were sorted as CD45.2<sup>-</sup>CD11b<sup>-</sup>O1<sup>-</sup>ACSA-2<sup>+</sup> population. For sorting of splenic stromal cells or red pulp macrophages, the cell suspension was subjected to immunomagnetic depletion of CD45<sup>+</sup> cells or positive selection of VCAM-1<sup>+</sup> cells using MACS (Miltenyi Biotec).

### qPCR detection of latent MCMV genomes

Total DNA was extracted from brain tissue or sorted cells using AllPrep DNA/RNA Micro Kit (Qiagen, #80204). MCMV and mouse genome copies were quantified as described previously [22, 23]. Viral gB and mouse Pthrp sequences were assayed in technical duplicates using 9  $\mu$ l of sample (200 ng DNA) per reaction. Serial dilutions of  $10^1$ - $10^6$  copies per reaction of the pDrive\_gB\_PTHrP\_Tdy plasmid were used to generate standard curves for both qPCR reactions. Quantitative PCR was performed using Fast Plus EvaGreen qPCR master mix (Biotium) in a 7500 Fast Real-Time PCR (Applied Biosystems). Cycling conditions were as follows: enzyme activation, 2 minutes (min) at 95°C, followed by 50 cycles of denaturation for 10 seconds (sec) at 95°C, annealing for 20 sec at 56°C and extension for 30 sec at 72°C. The specificity of amplified sequences was validated for all samples in each run by inspecting the respective melting curve profiles. Primer sequences that were used: Pthrp forward 5'-gggtatcgcctcatcgtctg-3' and reverse 5'-cgtttctcctcaccatctg-3'; gB forward 5'-gcagtctagtcgcttctgc-3' and reverse 5'-aaggcgtggactagcgataa-3'.

### Human fetal organotypic brain slice cultures

Human fetal organotypic brain slice cultures (hfOBSCs) were prepared as described previously [24]. The tissues obtained were anonymized and non-traceable to the donor. At the request by the researchers, only gender and gestational age are provided. Abortions were not performed for medical indications, and fetuses did not have any major anatomical deformities (checked by ultrasound prior to the procedure) or trisomy. The procedure was performed by *in utero* dissection and removal of fetal tissue specimens did not enable recovery of intact organs. Brain tissue fragments (approximately 0.5  $\times$  0.5 cm in size) were cut into 350  $\mu$ m thick slices using a vibratome (Leica, #VT1200S) in artificial cerebrospinal fluid (aCSF) (prepared in house) under constant oxygenation (95% O<sub>2</sub>, 5% CO<sub>2</sub>). Brain slices were transferred to 12-mm Transwells with polyester membrane inserts (0.4  $\mu$ m pore size; Corning, #3470) and recuperated for 1 h in recovery medium that was composed of a 7:3 (v/v) mixture of Neurobasal media and advanced DMEM/F12 culturing medium (both Life Technologies) supplemented with 20% heat-inactivated fetal bovine serum (FBS; Sigma, cat: F7524, lot: 0001644044) and antibiotics. After 1-h incubation in a CO<sub>2</sub> incubator at 37 °C, the recovery medium was replaced with optimized hfOBSC serum-free culture medium consisting of a 7:3 (v/v) mixture of Neurobasal media (Gibco, #21103049) and advanced DMEM/F12 culturing medium (Gibco, #12634010), B27 (2% v/v, Gibco, #17504044), N2 (1% v/v, Gibco, #17502048), glutaMAX (1% v/v, Gibco, #35050061), primocin, 1:500, Invivogen, #ant-pm-05), TGF- $\beta$ 2 human (2 ng/mL,

ProspecBio, #CYT-441), cholesterol (1.5  $\mu$ g/mL, Sigma Aldrich, #C3045), human recombinant m-CSF (100 ng/mL, Peprotech, #300-25), BDNF (50  $\mu$ g/mL, Peprotech, #450-02), NT-3 (10 ng/mL, Peprotech, #450-03), FGF2 (10 ng/mL, R&D Systems, #233-FB) and EGF (10 ng/mL, R&D Systems, #236-EG). The culture medium was refreshed every 48 h. The hfOBSCs were infected with  $10^7$  PFU of cell-free KL7-EGFP HCMV. After 1-h incubation at 37 °C, the inoculum was removed, and the brain slices were washed with PBS and subsequently maintained in the culture medium for 48 hours post-infection (hpi) at 37 °C in a CO<sub>2</sub> incubator. Additionally, one group of brain slices was treated with 1,000 U/ml of recombinant human IFN- $\gamma$  (Peprotech, #300-02) for 48 h. At the indicated time point, the hfOBSCs were fixed in PBS containing 4% paraformaldehyde and embedded in paraffin for histological analyses. For immunofluorescent staining, brain slices were treated with TrueBlack (Biotium, #23007) after citrate buffer antigen retrieval to decrease autofluorescence. The following primary antibodies were used for IF: FITC goat anti-GFP (1:250, Abcam, #ab6662) and rabbit anti-NeuN (1:500, Abcam, #ab177487). Unconjugated primary antibodies were labeled with the appropriate secondary antibody from donkey anti-rabbit IgG conjugated to AF555 (1:250, Invitrogen, #A-31572). Nuclei were stained with Hoechst 33342 Solution (Thermo Scientific, #62249). Images were taken using a Leica Stellaris 5 Low Incidence Angle confocal microscope.

### Statistical analyses

Statistical analyses were performed with Prism 5 (GraphPad Software Inc.). Appropriate statistical tests were employed depending on the number of animals per group and data distribution (Student's t-test, Mann-Whitney two-tailed test, Kruskal-Wallis test). A level of  $p < 0.05$  was considered to be statistically significant.

## Results

### Hippocampus is a major site of productive and latent MCMV infection

During congenital HCMV infection, the virus is detected in different brain regions, with the highest viral load and number of infected cells found in the fetal hippocampus [25]. To correlate these findings to the mouse model, we infected newborn C57BL/6 mice *i.p.* and harvested brains at multiple time points corresponding to different stages of acute MCMV infection in the brain. MCMV replication in the brain of mice infected as newborns starts around 7 dpi and peaks between 10 and 14 dpi, followed by the resolution of productive infection [10, 26]. The hippocampus, cortex, and cerebellum were isolated from each mouse brain, and viral load was then determined in each brain region using standard plaque assay

(Fig. 1A). At 14, 17, and 21 dpi, the highest MCMV load was detected in the hippocampus, analogous to observations in brains of cHCMV cases [25]. To identify the CNS cell types infected with MCMV, we performed immunohistochemical analysis on brain tissue 11 days post-infection. MCMV was infecting astrocytes (GFAP-positive cells), microglia (IBA1-positive cells), and mature neurons (MAP2-positive cells) (Fig. 1B) [27]. Again, this data closely mimics the prevalence of HCMV-infected cell types in post-mortem brain specimens of cHCMV cases [28].

The state of latency is defined as the persistence of CMV genomic DNA without the production of virus progeny [29]. Following infection of newborn mice, MCMV establishes latent infection in the brain and other organs of mice in the period between one and two months p.i., as evidenced by the lack of infectious virus and IE1-expression in tissue sections [10, 30]. Thus,

we quantified MCMV DNA in brain regions during the latent phase of infection (180 dpi) using qPCR. MCMV genomes were detected in all tested brain regions, with the highest viral DNA levels again observed in the hippocampus, followed by the cortex and lastly, the cerebellum (Fig. 1C). Notably, this data correlated with the viral loads in the respective brain regions detected during acute infection (Fig. 1A). Overall, MCMV has a broad cell tropism in the CNS, with a particular propensity to infect and establish latency in the hippocampus.

**Neurons are the main source of infectious virus during the late phase of acute infection**

To determine which cells produce infectious virus within the CNS, we used a recombinant reporter virus MCMV-flox that encodes the enhanced green fluorescent protein (EGFP) preceded by a floxed stop sequence. Thus, EGFP expression is activated by the Cre recombinase.

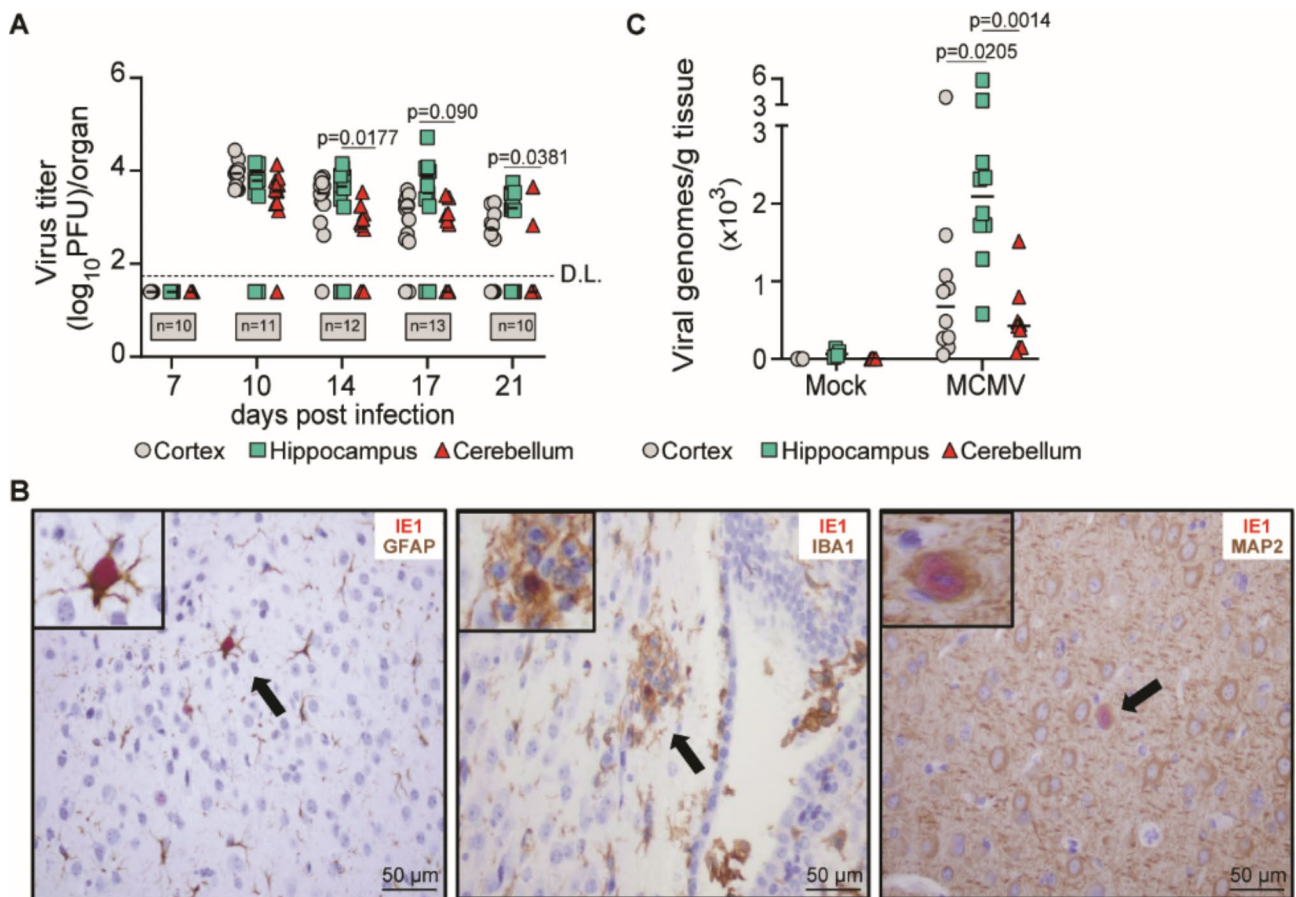


**Fig. 1** Tropism of mouse cytomegalovirus in the brain. **A-C** Newborn C57BL/6 mice were infected with MCMV. **A** Viral titers in the cortex, hippocampus, and cerebellum were determined by plaque assay at the indicated days post-infection (dpi) (n=10–13 mice/time point). Results for individual mice are shown (circles, squares, and triangles). Black horizontal lines indicate the median values. D.L., detection limit. Kruskal–Wallis test was used. **B** GFAP (astrocyte marker), IBA1 (microglia marker) or MAP2 (neuron marker, all cells stain brown) and MCMV IE1 protein (red) co-staining of paraffin-embedded brain sections on 11 dpi. Arrows point to MCMV-infected cells. Representative images are shown (40x magnification, 100x magnification insert). **C** MCMV genome-equivalent copy numbers per gram of tissue in indicated brain regions determined by qPCR at 180 dpi (n=10 mice/time point). Mock, mock-infected mice. Results for individual mice are shown (circles, squares, and triangles). Black horizontal lines indicate the median values. D.L., detection limit. Kruskal–Wallis test was used. p values indicate statistically significant differences

By infecting transgenic mice expressing Cre under the control of a brain cell type-specific promoter, the virus undergoes Cre-mediated recombination only in cells expressing Cre and further disseminates as EGFP-positive (EGFP<sup>+</sup>) virus (Fig. 2A) [31]. We have i.p. infected newborn mice in which Cre is selectively expressed in astrocytes (GFAP-Cre<sup>+/-</sup> mice), microglia (Sall1-Cre-ERT2<sup>+/-</sup> mice), neurons (BAF53b-Cre<sup>+/-</sup> mice), as well as respective Cre-negative littermate controls. The Cre-ERT2 transgenic line received tamoxifen (TAM) treatment on three subsequent days within the first postnatal

week (Fig. S1A). High efficiency of TAM-induced recombination was confirmed by crossing Sall1-Cre<sup>+/-</sup>/ERT2 mice with reporter Rosa26-loxP-tdTomato (R26<sup>tdTomato</sup>) mice (Fig. S1B).

Brain and peripheral organs were harvested at 7, 10, 14, and 17 dpi. The number of reporter-tagged and untagged infectious viruses in organ homogenates of transgenic mice and littermate controls was determined by plaque assays and confocal microscopy (Fig. 2B). The results obtained by infecting GFAP-Cre<sup>+/-</sup> transgenic mice revealed that astrocytes are the major brain cell type

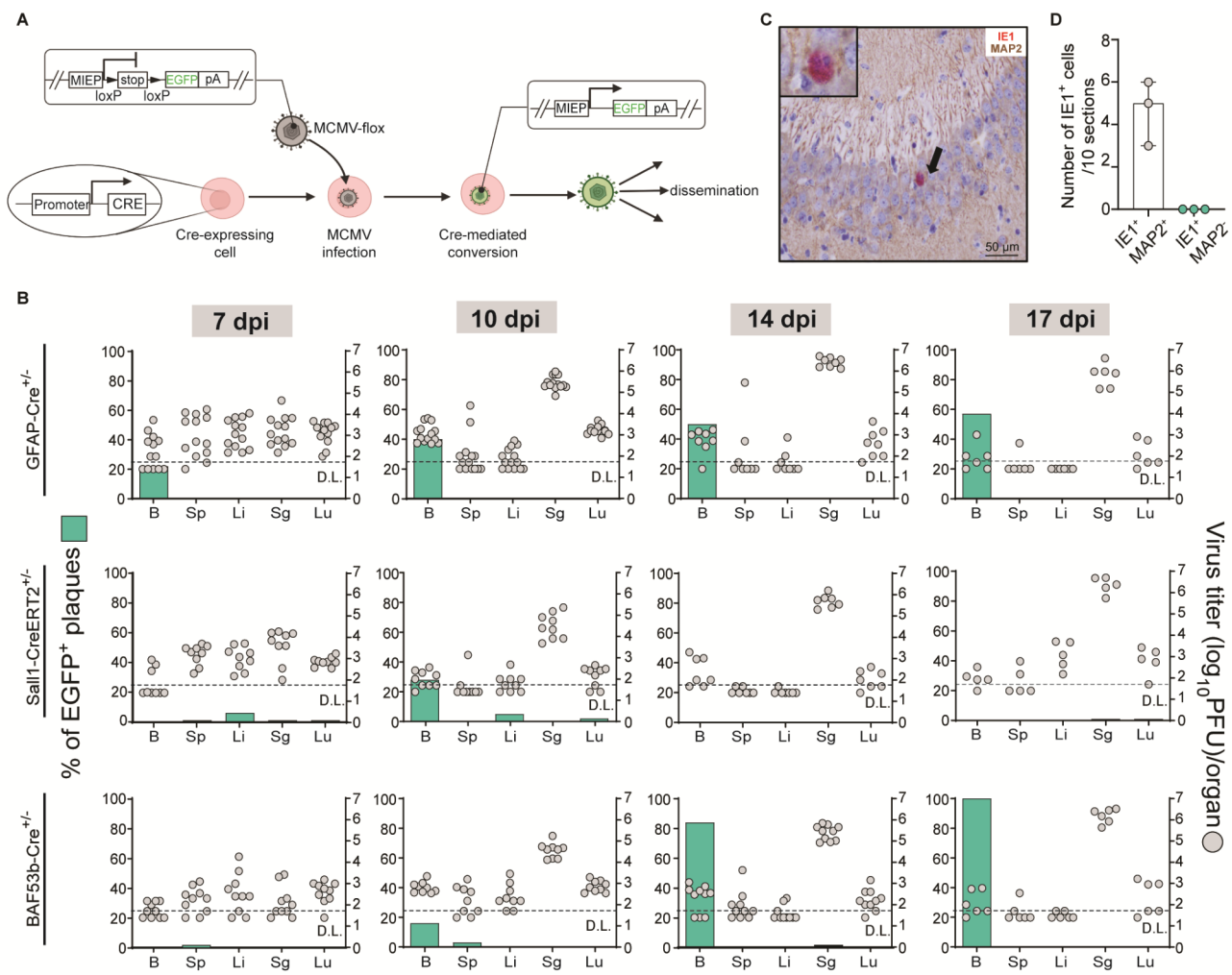


**Fig. 2** Neurons are the major source of infectious virus during the late phase of acute infection in the brain. **A** Schematic representation of the reporter system for quantitative tracking of virus progeny in vivo. Following infection of a Cre-expressing cell with MCMV-flox, the loxP-flanked (floxed) STOP cassette is removed from the viral genome, allowing constitutive EGFP expression under the control of the major immediate early promoter (MIEP) of HCMV. **B** Newborn GFAP-Cre<sup>+/-</sup>, Sall1-CreERT2<sup>+/-</sup> and BAF53b-Cre<sup>+/-</sup> transgenic mice were infected i.p. with MCMV-flox. Tamoxifen (TAM) was administered for 3 consecutive days intragastrically to Sall1-CreERT2<sup>+/-</sup> mice. Mice were euthanized at 7, 10, 14, and 17 dpi, and organs were collected. Titrations in brain (B), spleen (Sp), liver (Li), salivary glands (Sg) and lungs (Lu) of individual mice are shown (circles). Mean percentage of EGFP<sup>+</sup> plaques per organ are shown (bars). D.L., detection limit. **C** Representative MAP2 (brown) and MCMV IE1 (red) co-staining of paraffin-embedded brain sections on 17 dpi. Arrows point to MCMV-infected cells. Representative MCMV-infected neuron in the hippocampus is shown (40x magnification, 100x magnification insert). **D** Quantification of IE1 protein-positive MAP2 neurons. Columns indicate median values (n=3 mice, 10 sections/mouse)

producing infectious virus, given that reporter virus conversion occurs as early as 7 dpi. Furthermore, less than 60% of virus replicating in the brain has originated from astrocytes at any time point of infection, suggesting that the virus can enter the brain without infecting blood-brain barrier astrocytes (Fig. 2B). Microglia-derived virus was detected on 10 dpi, but not on other time points, suggesting that microglia-derived virus does not readily spread to other cells. Infection of BAF53b-Cre<sup>+/-</sup> mice showed that mature neurons are not the initial targets during the acute phase of MCMV infection in the brain, as no and <20% of viruses were neuron-derived at 7 and 10 dpi, respectively. Notably, neurons became the major cell type producing infectious virus at later time points (Fig. 2B). This observation was validated by histological quantification of MCMV-infected cells (IE1<sup>+</sup> cells) in the brains of C57BL/6 mice infected with wild-type MCMV. MCMV-infected cells were exclusively MAP2<sup>+</sup> neurons on 17 dpi (Fig. 2C and D), thereby providing independent confirmation of the data obtained using the reporter system (Fig. 2B). We did not observe EGFP<sup>+</sup> plaques in peripheral organs of GFAP-Cre<sup>+/-</sup> and BAF53b-Cre<sup>+/-</sup> mouse lines, suggesting that the virus does not spread from the CNS back to the periphery. We observed some conversion in the peripheral organs of Sall1CreERT2<sup>+/-</sup> mice, which was in line with the known expression of Sall1 in several macrophage populations [32]. Importantly, we did not observe EGFP<sup>+</sup> plaques in MCMV-flox-infected Cre-negative littermate controls, indicating that no conversion of MCMV-flox occurred in the absence of Cre (Fig. S1C). Altogether, our findings demonstrate that MCMV productively infects multiple brain-resident cell types, of which neurons are the dominant source of MCMV during the late phase of acute infection.

#### CD4<sup>+</sup> T-cells are required to resolve productive infection in cortical and hippocampal neurons

During acute MCMV infection, CD8<sup>+</sup> and CD4<sup>+</sup> T-cells infiltrate the brain and contribute to virus control (8,30). Since T-cells infiltrate the brain only at about 10 dpi (8), our data suggest that the T-cell-mediated control of virus infection in neurons is delayed compared to other cell types (Fig. 2B, C and D). To determine the T-cell subset involved in resolving the productive infection in neurons, we infected newborn wild-type C57BL/6, CD4<sup>-/-</sup> (CD4<sup>-/-</sup>) and CD8-deficient (CD8<sup>-/-</sup>) mice by the i.p. route with MCMV. Brain and peripheral organs were harvested at 14, 30, and 70 dpi. We did not observe significant differences in both body weight and survival of MCMV-infected mice that lack CD4<sup>+</sup> or CD8<sup>+</sup> T-cells compared to wild-type C57BL/6 mice (Fig. S22A and B). Notably, mice lacking CD4<sup>+</sup> T-cells had significantly higher viral titers at 14 dpi onwards and could not resolve productive infection in the brain (Fig. 3A). Even at 120

dpi, replicating MCMV was still detectable in brains of CD4<sup>-/-</sup> mice (Fig. 3B). In contrast, CD8<sup>+</sup> T-cells were not essential for the resolution of productive MCMV infection in the brain (Fig. 3A). In agreement with MCMV infection in adult mice [33], CD4<sup>+</sup> T-cells were not essential for the resolution of productive infection in other peripheral organs, including the spleen and lungs, but were required in salivary glands (Fig. S2C, D and E).

To define if CD4<sup>+</sup> T-cells are pivotal in controlling MCMV infection in neurons, brains from CD4<sup>-/-</sup> mice were collected at 37 dpi for immunohistochemical detection of MCMV-infected cells (IE1<sup>+</sup> cells). The viral IE1 protein was mainly detected in the cortex and hippocampus (Fig. 3C), where MAP2<sup>+</sup> cells (neurons) were the predominant MCMV-infected cell type (Fig. 3D and E). Only a few GFAP<sup>+</sup> astrocytes were infected, while we did not detect infected IBA1<sup>+</sup> microglia (Fig. 3E, G and H). Therefore, our results strongly suggest that CD4<sup>+</sup> T-cells are essential to control MCMV infection in neurons. Altogether, we show that CD4<sup>+</sup> T-cells, not CD8<sup>+</sup> T-cells, are necessary to terminate productive MCMV infection and the subsequent establishment of latency in the brain.

#### Resolution of productive MCMV infection in neurons is dependent on IFN- $\gamma$ and IL-12

CD4<sup>+</sup> T-cells possess many antiviral functions, from regulating antiviral immunity mediated by other cell types to directly suppressing viral replication in infected cells [34]. To elucidate the mechanism of CD4<sup>+</sup> T-cell-mediated control of MCMV infection in the brain, we infected knockout mice that lack critical elements of T-cell effector functions. First, the role of cytotoxic mechanisms was determined by infecting newborn mice that lack the cytolytic proteins perforin (Prf1<sup>-/-</sup>) or granzymes A and B (Gzma<sup>-/-</sup>Gzmb<sup>-/-</sup>). Compared to wild-type C57BL/6 controls, no significant differences were observed in viral titers of Prf1<sup>-/-</sup> or Gzma<sup>-/-</sup>Gzmb<sup>-/-</sup> mice, suggesting that non-cytolytic T-cell mechanism controls MCMV infection in neurons (Fig. 4A and B). As expected, perforin and granzymes A and B were necessary to control MCMV in the lungs and salivary glands at 14 and 30 dpi (Fig. S3A and B) [35, 36]. Next, we tested the outcome of MCMV infection in Tumor Necrosis Factor Receptor p55 (TNFRp55) (TNFRp55<sup>-/-</sup>) and IFN- $\gamma$  (IFN- $\gamma$ <sup>-/-</sup>) knockout mice. The TNFRp55<sup>-/-</sup> mice had modest but significantly increased viral titers in the brain compared to WT control mice at 30 dpi, while the majority of animals resolved productive infection in the brain by 70 dpi (Fig. 4C). The same was observed in the lungs, as TNFRp55<sup>-/-</sup> mice cleared MCMV infection with a delayed kinetic compared to C57BL/6 controls, while no difference was observed in the spleen and salivary glands (Fig. S3C). In contrast, IFN- $\gamma$ <sup>-/-</sup> mice displayed increased virus titers of nearly two orders of magnitude

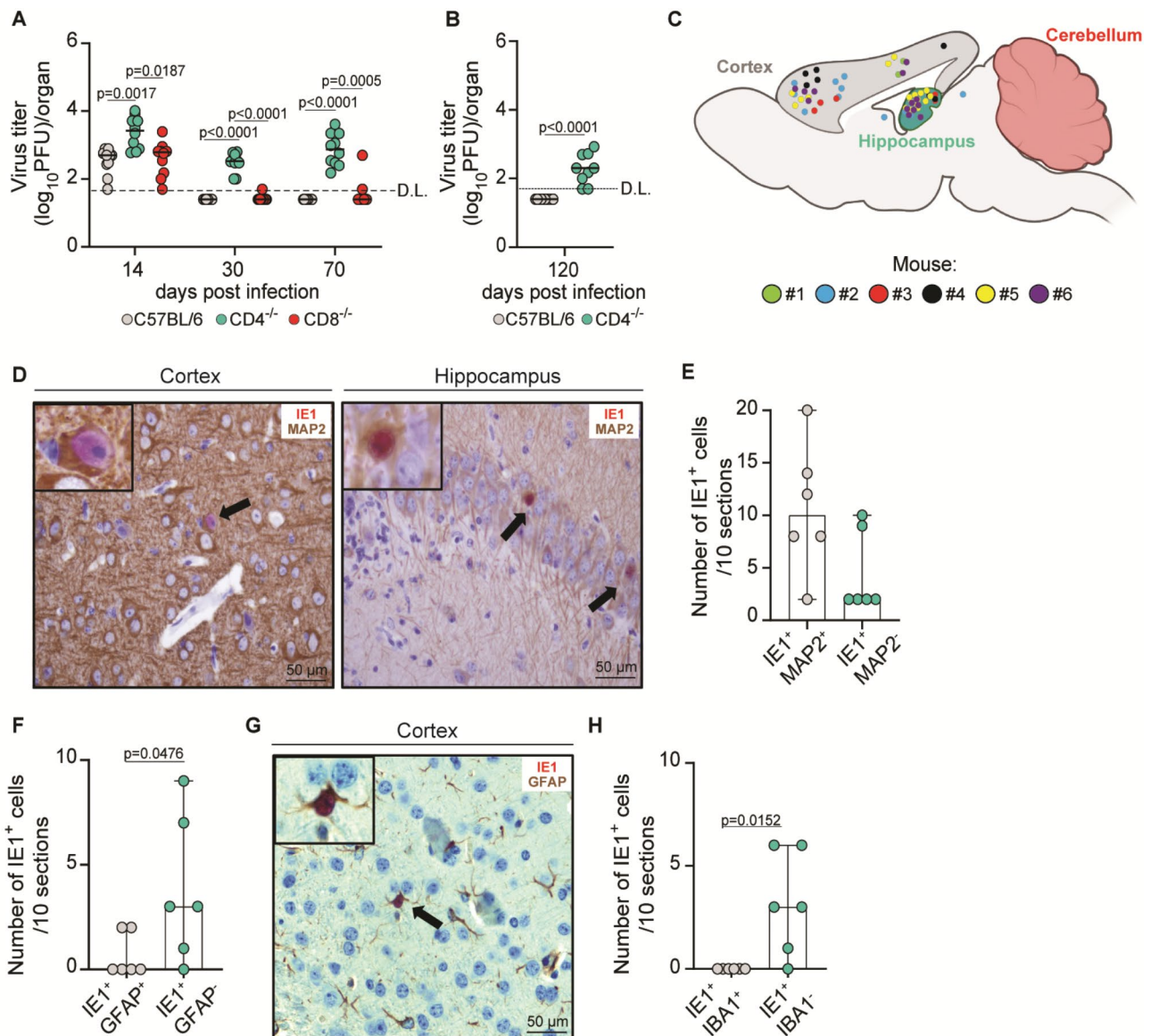


**Fig. 3** CD4<sup>+</sup> T-cells are essential for the resolution of productive MCMV infection in neurons. **A–B** Newborn wild-type C57BL/6, CD4<sup>-/-</sup> (CD4<sup>-/-</sup>) and CD8<sup>-/-</sup> (CD8<sup>-/-</sup>) mice were infected i.p. with MCMV. Viral titers in the brain ( $n = 10$  mice) were determined on **A** 14, 30, 70, and **B** 120 dpi. Titers in brains of individual mice are shown (circles). Black horizontal lines indicate the median values. D.L., detection limit. **A** Kruskal–Wallis test and **B** Mann–Whitney two-tailed test were used. **C–H** Immunohistochemical analysis of MCMV infection in neurons, astrocytes and microglia of CD4<sup>-/-</sup> mice at 37 dpi ( $n = 6$  mice, 10 sections/mouse). **C** A simplified 2D sagittal view of the location of IE1<sup>+</sup> cells in the brain regions. Each colored dot represents individual IE1<sup>+</sup> cells in six individual mice. **D** Representative MAP2 (neuron marker, brown) and MCMV IE1 (virus infection, red) co-staining of paraffin-embedded brain sections. Arrows point to the MCMV-infected neurons (40x magnification, 100x magnification insert). **E** Quantification of IE1<sup>+</sup>MAP2<sup>+</sup> neurons in the brain. **F** Quantification of IE1<sup>+</sup>GFAP<sup>+</sup> astrocytes in the brain. **G** Representative GFAP (astrocyte marker, brown) and MCMV IE1 (virus infection, red) co-staining of paraffin-embedded brain sections. Arrow points to the MCMV-infected astrocyte (40x magnification, 100x magnification insert). **H** Quantification of IE1<sup>+</sup>IBA1<sup>+</sup> microglia in the brain. **E–F, H** Columns indicate median values. Mann–Whitney two-tailed test was used. p values indicate statistically significant differences

and were not able to resolve brain infection even by 70 dpi (Fig. 4D). A similar effect was observed in salivary glands, previously described to require IFN- $\gamma$  to control productive infection (Fig. S3D) [37]. Histological analysis of brains from IFN- $\gamma$ -deficient animals at 37 dpi showed the same pattern of MCMV infection (Fig. 4E), as observed in CD4<sup>+</sup> T-cell deficient animals (Fig. 3C).

Again, MCMV-infected cells were predominantly found in the cortex and hippocampus (Fig. 4E, Fig. S3E), and MAP2<sup>+</sup> neurons were the main infected population of cells in IFN- $\gamma$ <sup>-/-</sup> mice (Fig. 4F and G).

Interleukin-12 (IL-12) is a pro-inflammatory cytokine important for T helper 1 (Th1) cell differentiation [38]. Thus, we infected IL-12 receptor subunit beta 2 deficient

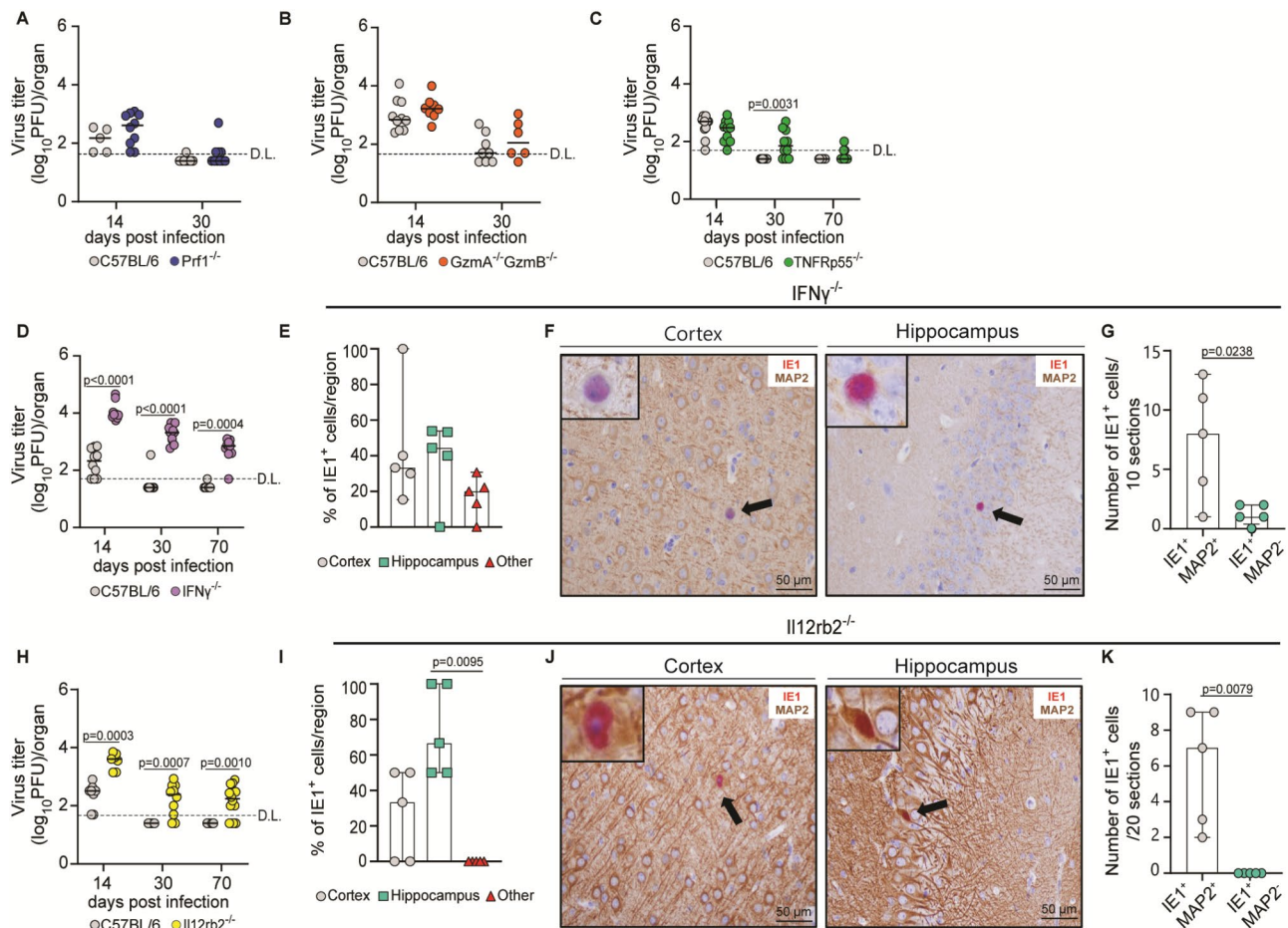


**Fig. 4** IFN- $\gamma$  and IL-12 promote the resolution of productive MCMV infection in neurons. Newborn C57BL/6, **A** Prf1<sup>-/-</sup>, **B** GzmA<sup>-/-</sup>GzmB<sup>-/-</sup>, **C** TNFRp55<sup>-/-</sup>, **D-G** IFN- $\gamma$ <sup>-/-</sup>, and **H-K** Il12rb2<sup>-/-</sup> mice were infected with MCMV on PND1. **A-D, H** Viral titers in the brain were determined by plaque assay at 14, 30 and 70 dpi ( $n = 5-14$ ). Titers in organs of individual mice are shown (circles). Black horizontal lines indicate the median values. D.L., detection limit. Mann-Whitney two-tailed test was used. **E-G, I-K** Immunohistochemical staining of MCMV infection in neurons at day 37 p.i. in **E-G** IFN- $\gamma$ <sup>-/-</sup>, and **I-K** Il12rb2<sup>-/-</sup> mice. **E, I** Localization of IE1 protein-positive cells in the murine brain. Median values are shown ( $n = 5$ , 10 sections/mouse). Other refers to IE1<sup>+</sup> cells outside the cortex and hippocampus in the brain. Kruskal-Wallis test was used. **F, J** Representative images of MCMV infected MAP2<sup>+</sup> neuron. Arrows point to the MCMV-infected neurons (40x magnification, 100x magnification insert). **G, K** Quantification MCMV infected MAP2<sup>+</sup> neurons ( $n = 5$  mice,  $G = 10$  sections/mouse,  $K = 20$  sections/mouse). Columns indicate median values. Mann-Whitney two-tailed test was used. p values indicate statistically significant differences

(Il12rb2<sup>-/-</sup>) mice, which exhibit markedly reduced IFN- $\gamma$  responses in various infection and injury models [38–40]. Analogous to IFN- $\gamma$ <sup>-/-</sup> mice, Il12rb2<sup>-/-</sup> mice could not resolve MCMV infection in the brain (Fig. 4H). MCMV was detected predominantly in the cortex and hippocampus (Fig. 4I, Fig. S3F), and exclusively within MAP2<sup>+</sup> neurons (Fig. 4J and K). In conclusion, these findings show the crucial role of IFN- $\gamma$  and IL-12 signaling, but not perforin and granzyme-mediated cytotoxicity, to control productive MCMV infection of neurons.

#### IFN- $\gamma$ inhibits HCMV infection of human neurons

Since IFN- $\gamma$  was critical for controlling MCMV infection in mouse neurons, we hypothesized that the same might be true for HCMV infection in human neurons. To test this hypothesis, we infected either the human

neuroblastoma SH-SY5Y cell line [42], or human fetal organotypic brain slice cultures (hFOBSCs) with KL7-EGFP HCMV, a recombinant HCMV expressing GFP under the control of a truncated major immediate-early promoter. Treatment of SH-SY5Y cells with recombinant IFN- $\gamma$  either prior to (Fig. 5A and B, Fig. S4A) or following (Fig. 5C and D, Fig. S4B) infection with KL7-EGFP HCMV significantly decreased the number of EGFP-positive SH-SY5Y cells in a dose-dependent manner. Next, to model the neuropathology of congenital HCMV infection, we infected hFOBSCs with KL7-EGFP HCMV, in a manner similar to the recently reported model for herpes simplex virus (HSV) infection [24]. Not only did the KL7-EGFP HCMV efficiently infect cells within the hFOBSCs (Fig. 5E, Fig. S4C), but treatment of hFOBSCs with IFN- $\gamma$  decreased the number of KL7-EGFP HCMV-infected

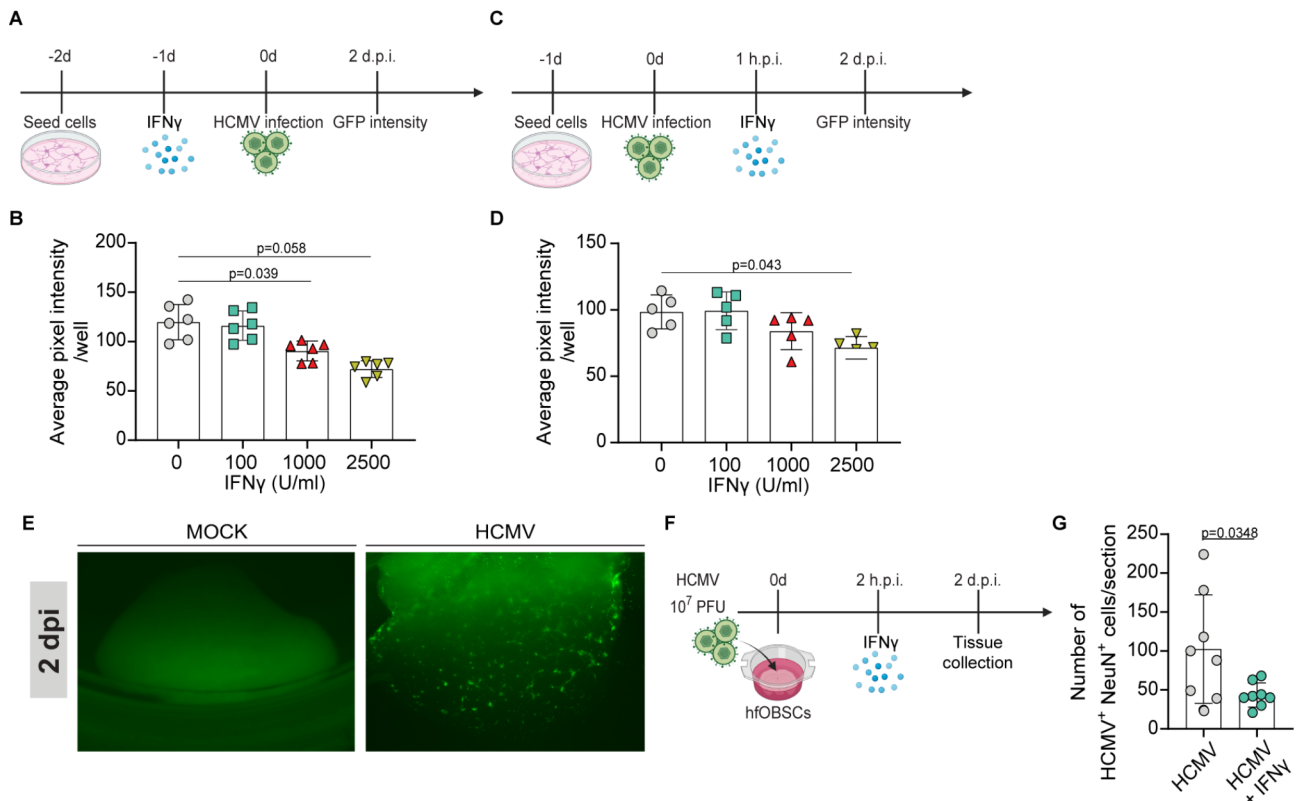


**Fig. 5** IFN- $\gamma$  inhibits HCMV infection of human neurons. **A** The experimental system for **B**. SH-SY5Y cells were treated with recombinant IFN- $\gamma$ . The following day, cells were infected with 10 MOI of KL7-EGFP HCMV and at 2 dpi EGFP fluorescence was recorded and expressed as an average 8-bit green channel pixel intensity for each well. **B** Quantification of EGFP fluorescence. The data are merged from two independent experiments, with three technical replicates in each experiment. Unpaired two-tailed Student’s test was used. **C** Experimental scheme for **D**. SH-SY5Y cells were infected with 10 MOI of KL7-EGFP HCMV. One hour post-infection, cells were treated with recombinant IFN- $\gamma$  and at 2 dpi EGFP fluorescence was recorded and expressed as an average 8-bit green channel pixel intensity for each well. **D** Quantification of EGFP fluorescence. The data are merged from two independent experiments, with three technical replicates in each experiment. Unpaired two-tailed Student’s test was used. **E** hFOBSCs were infected with KL7-EGFP HCMV. Fluorescent microscopy monitoring of GFP expression in the hFOBSC at 2 dpi **F** Schematic representation of human brain slice cultures either untreated or treated with IFN- $\gamma$ , and subsequently infected with HCMV. **G** hFOBSCs were infected with KL7-EGFP HCMV. One group of brain slices was treated with 1000 U/ml of recombinant IFN- $\gamma$ . Brain slices were collected 2 dpi. HCMV<sup>+</sup> NeuN<sup>+</sup> cells were quantified. Mean values  $\pm$  SD are shown ( $n=2$  donors, 4 section/condition/donor). Unpaired two-tailed Student’s test was used.  $p$  values indicate statistically significant differences

NeuN<sup>+</sup> neurons, demonstrating the neuroprotective role of IFN- $\gamma$  against HCMV infection (Fig. 5F and G, Fig. S4D). Overall, these data show that IFN- $\gamma$  inhibits HCMV infection in human neurons.

**Neurons are sites of MCMV latency and reactivation**

Despite the resolution of productive infection, MCMV still establishes life-long latency in the brain [10]. However, the cellular sites of MCMV latency in the brain remain unclear. To identify which cell types harbor the latent virus, we used a recombinant virus MCMV-GFP\_Cre that codes for simultaneous co-expression of GFP and Cre-recombinase under HCMV major immediate-early promoter (MIEP) (Fig. S5A). We infected newborn Rosa26-loxP-tdTomato (R26<sup>tdTomato</sup>) reporter mice, which have a loxP-flanked STOP cassette preventing the expression of tdTomato fluorescent protein. Thus, infection of cells with MCMV-GFP\_Cre enables tdTomato expression

following Cre-mediated recombination. Brains of latently MCMV-GFP\_Cre-infected mice were collected at 45 dpi and analyzed for the expression of tdTomato reporter protein by confocal microscopy. Interestingly, tdTomato-positive cells displayed a neuronal morphology, which strengthens the notion that neurons are the major cell type infected during the late phase of productive MCMV infection (Fig. 6A). By using the neuronal marker NeuN, we confirmed that tdTomato is expressed exclusively in neurons but not in astrocytes or microglia (Fig. 6B and C), suggesting that MCMV established a latent infection in neurons. Accordingly, we could not detect MCMV genomes in sorted astrocytes and microglia by qPCR (Fig. S5B, C and D). As shown in Fig. 1B, the hippocampus is the dominant site of MCMV latency in the brain. To test if MCMV can reactivate in the hippocampus and other brain regions, we isolated different brain regions from latently infected mice and cultured these

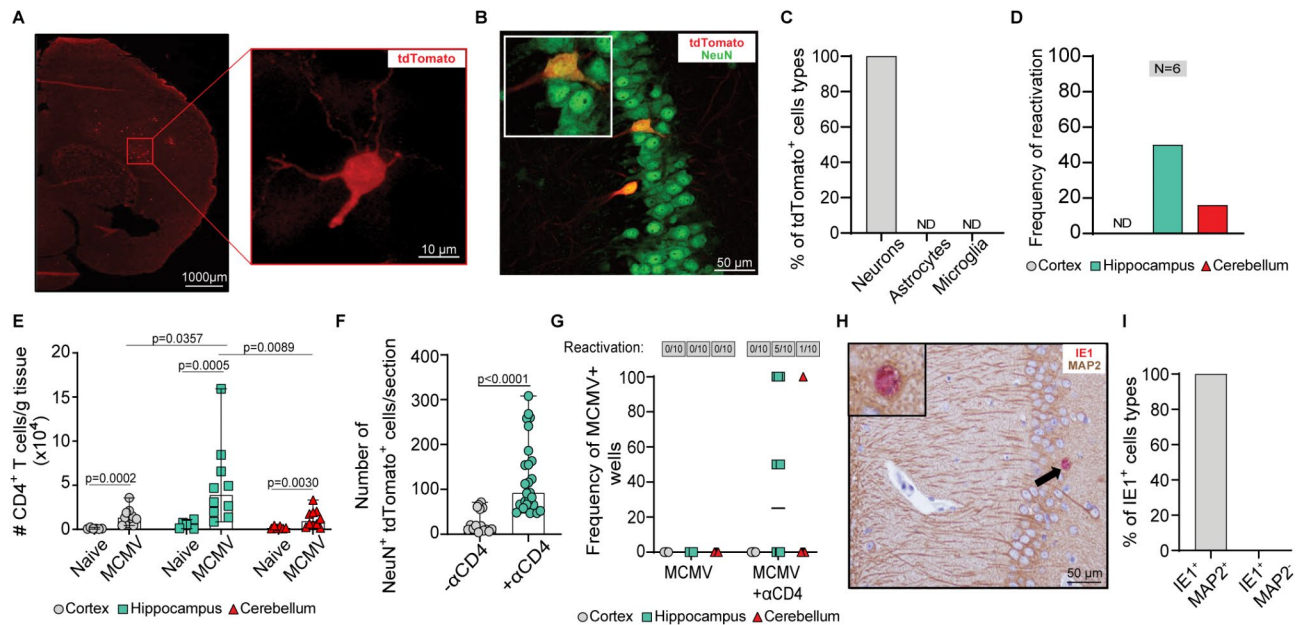


**Fig. 6** Neurons are the sites of latent and reactivating MCMV in the CNS. **A–C, F** Newborn R26<sup>tdTomato</sup> mice were infected with MCMV-GFP-Cre i.p. **A** Brains were collected and analyzed 45 dpi. A representative brain section (10x magnification) containing tdTomato-positive cells (left) and representative magnified (63x magnification) tdTomato-positive cell (right) are shown. **B** Representative image of tdTomato-positive NeuN<sup>+</sup> neuron (40x magnification). **C** Quantification of cell types expressing tdTomato reporter protein 45 dpi (n=5 mice, 5 sections/mouse). ND - Not detected. **D** Newborn C57BL/6 mice were infected with MCMV. Brain regions were isolated and cultured ex vivo for 6 weeks. The reactivation frequency in indicated brain regions was determined (n=6 mice). ND - not detected. **E** Newborn C57BL/6 mice were infected with MCMV. The number of CD4<sup>+</sup> T-cells per gram of tissue was analyzed using flow cytometry at 180 dpi. Columns indicate median values (n=6–10 mice). Kruskal–Wallis test was used. **F** Mice were depleted of CD4<sup>+</sup> T-cells starting on 90 dpi for 1 month. Mice were perfused, sacrificed and brains were collected and frozen. Quantification of co-expression of NeuN and tdTomato is shown (n=3–5 mice, 5 sections/mouse). Columns indicate median values. Mann–Whitney two-tailed test was used. **G** Newborn C57BL/6 mice were infected with MCMV and mice were depleted of CD4<sup>+</sup> T-cells starting at 90 dpi for 1 month (n=10 mice). Brain regions were separated, homogenized and layered on MEF cells in multiwell plates. The frequency of MCMV-positive wells was determined. Results for individual mice are shown (circles, squares and rectangles). The number of mice from which the virus was recovered is indicated above the graph. **H–I** Newborn C57BL/6 mice were infected with MCMV and mice were depleted of CD4<sup>+</sup> T-cells starting on 90 dpi for 1 month. **H** Representative image of MCMV-infected MAP2<sup>+</sup> neuron. The arrow points to the MCMV-infected neuron (40 magnification, 100x magnification insert). **I** Quantification of IE1 protein-positive MAP2 neurons (n=4 mice, 20 sections/mouse). p values statistically indicate significant differences

specimens as ex vivo explants for 6-weeks. In accordance with latent genome loads (Fig. 1B), the hippocampus was the prime site of MCMV reactivation in tissue explants (Fig. 6D). Active viral replication was absent in the mice from which we collected tissue, as no infectious virus was detected in their salivary glands (Fig. S5E).

We showed that CD4<sup>+</sup> T-cells are critical to suppress productive infection in the brain (Fig. 3). To analyze the distribution of CD4<sup>+</sup> T-cells in the latently infected brain regions, we performed flow cytometry analysis. The hippocampus harbored the highest frequency of CD4<sup>+</sup> T-cells (Fig. 6E), correlating with the number of latent genomes (Fig. 1B) and potential to reactivate the virus (Fig. 6D). To assess the role of CD4<sup>+</sup> T-cells in the control of latent MCMV in neurons, we depleted CD4<sup>+</sup> T-cells in latently infected R26<sup>tdTomato</sup> reporter mice infected with MCMV-GFP\_Cre. Depletion of CD4<sup>+</sup> T-cells resulted in a significant increase in number of tdTomato-positive neurons, suggesting viral reactivation and further spread among neurons following loss of CD4<sup>+</sup> T-cell-mediated

control (Fig. 6F). Finally, we depleted CD4<sup>+</sup> T-cells in latently infected C57BL/6 mice and isolated brain regions. Depletion efficiency of CD4<sup>+</sup> T-cells in the brain was confirmed by flow cytometry (Fig. S5F). In the control, non-depleted group, we did not detect reactivating virus. The highest frequency of MCMV reactivation was observed in the hippocampus, suggesting that the hippocampus is also the primary site of MCMV reactivation upon loss of CD4<sup>+</sup> T-cell-mediated control (Fig. 6G). MCMV reactivation was detected exclusively in neurons following depletion of CD4<sup>+</sup> T-cells (Fig. 6H and I). Overall, these data suggest that neurons are sites of MCMV latency and that CD4<sup>+</sup> T-cells are required to prevent reactivation.

## Discussion

HCMV is a leading infectious cause of congenital viral infections with limited treatment options [2], warranting a better understanding of the disease pathogenesis. We have previously shown that MCMV establishes latency in

the brain, with CD4<sup>+</sup> T-cells required to maintain CD8<sup>+</sup> T<sub>RM</sub> cells and virus control in the brain [30]. Here, we investigated MCMV dissemination, immune mechanisms resolving productive and controlling latent infection, and cellular sites of MCMV latency in the brain in a mouse model of cHCMV infection. We show that MCMV is preferentially localized in the hippocampus during acute infection and latency. Furthermore, we show that MCMV initially infects diverse cell types in the CNS. Still, neurons become the primary reservoir of MCMV during the late productive and the subsequent latent phase of infection. Mechanistically, we show that IL-12, CD4<sup>+</sup> T-cells and IFN- $\gamma$  are crucial at two different stages of MCMV infection of the brain. First, they all contributed to the control of productive MCMV infection in neurons, and later, they prevent the reactivation of latent virus in cortical and hippocampal neurons. Finally, we have confirmed the importance of IFN- $\gamma$  in protecting neurons from HCMV infection.

The highest HCMV load in the brain has been reported in the hippocampus of congenitally infected fetuses [25]. Similarly, we show that the hippocampus is the main region targeted by MCMV. High hippocampal preference has also been reported in a model of congenital guinea pig CMV infection [43]. However, it remains to be determined what the underlying mechanistic reason is for the preferential CMV infection of the hippocampus. Findings from animal studies demonstrate notable variations in the brain regions susceptible to different neurotropic viruses [44]. Preference for hippocampal infection has been reported for other viruses, including DNA viruses (e.g. herpesviruses) and RNA viruses (e.g. flaviviruses) [45, 46]. In the case of HSV-1, the preference for hippocampal infection has been related to the high expression of viral receptors, lower levels of antiviral cytokines, and a neurogenic niche [47]. Furthermore, neuronal populations differ between brain regions, which can determine their susceptibility to infection [47–49]. Moreover, microglia display regional heterogeneity in the brain, which could play a significant role in antiviral responses [51]. Finally, the hippocampus blood-brain barrier is more susceptible to insults than other brain regions, potentially enabling more efficient hematogenous virus spread [52].

Like HCMV [53], MCMV has a broad cell tropism in acutely infected brains. By following MCMV dissemination in the acutely infected brain, we have shown that astrocytes are initial targets and a substantial cellular source of infectious viruses. Astrocytes are often targets of neurotropic viral infections, including cHCMV infection, due to their anatomical location and morphological properties that support productive virus infection [28, 54]. Microglia were also infected with MCMV, particularly at the early stage of infection. However, the

microglia-derived virus does not readily spread to other cells, suggesting an efficient microglial mechanism for virus containment. Our observation fits with data for the infection of other tissue-resident macrophages, often infected with CMV, but are not major virus producers [55, 56]. For example, MCMV infects subcapsular sinus macrophages (SSMs) in the lymph nodes, which restrict viral spread and thereby protect other cells from infection [55]. At later time points of acute infection, the virus is cleared from microglia and astrocytes, and neurons become the primary source of infectious virus, demonstrating slower immune control of the virus in neurons.

In most viral brain infections studied, CD8<sup>+</sup> T-cells were shown to be critical for virus control [57]. Here, we have shown that CD4<sup>+</sup> T-cells are required to resolve productive MCMV infection in the brain. CD8<sup>+</sup> T-cells play a pivotal role in protecting against MCMV in most organs, except salivary glands, where the virus is controlled by CD4<sup>+</sup> T-cells [33]. In addition, CD4<sup>+</sup> T-cells provide compensatory protective activity in adult mice depleted of CD8<sup>+</sup> T-cells [58]. In cases of cHCMV infection, T-cells infiltrate the infected fetal brains [59, 60]. Higher numbers of CD8<sup>+</sup> T-cells in the brain correlated with increased disease severity [60]. Conversely, cHCMV cases with more severe sequelae at birth have significantly lower counts of CD4<sup>+</sup> T-cells [61]. In contrast to infected adults, infants with cHCMV have long-term impaired CD4<sup>+</sup> T-cell response, but not CD8<sup>+</sup> T-cell response, demonstrating the importance of early-life CD4<sup>+</sup> T-cell-mediated immunity to HCMV [62, 63]. Adult patients with human immunodeficiency virus (HIV) and HCMV co-infection have neurotropic HCMV infections when the number of CD4<sup>+</sup> T-cells is particularly low [64, 65]. The protective role of CD4<sup>+</sup> T-cells has also been reported in the rhesus macaque model of congenital rhesus CMV infection and a guinea pig CMV model of congenital infection [66, 67]. Thus, the importance of CD4<sup>+</sup> T-cells in congenital CMV infection in humans, non-human primates, and other rodents aligns with our findings obtained in the mouse model of congenital infection.

The resolution of productive MCMV infection in neurons does not depend on cytolytic mechanisms. This is unsurprising, as cytolytic mechanisms may cause neuronal death [68]. Cytolytic mechanisms are more important for the clearance of viral infections from glial cells [44]. We show that IFN- $\gamma$  is critical for controlling MCMV infection and limits the establishment of viral latency in neurons. Accordingly, brain CD4<sup>+</sup> T-cells express markers of tissue residency and exert Th1 phenotype, expressing CD11a, T-bet, and CXCR3, and producing IFN- $\gamma$  when stimulated with macrophages pulsed with MCMV antigens [30]. Previous studies have shown that IFN- $\gamma$  is necessary to control several other virus infections in the

brain [68–72]. During HSV-1 infection, CD8<sup>+</sup> T-cells control HSV-1 latency in trigeminal ganglia by blocking viral reactivation via IFN- $\gamma$  [74]. CD4<sup>+</sup> T-cells are not directly involved in the control of HSV-1 latency in trigeminal ganglia, but rather mediate early CD8<sup>+</sup> T-cell priming to generate an efficient local effector memory CD8<sup>+</sup> T-cell population [75]. However, here we show that CD8<sup>+</sup> T-cells are not critical for controlling MCMV infection in the brain. This finding resembles the control of MCMV infection in salivary glands, where the resolution of productive infection does not rely on CD8<sup>+</sup> T-cells. To support the data on Th1-dependent infection control in neurons, we have shown that animals lacking IL-12 receptors, and thus exhibiting markedly reduced IFN- $\gamma$  production [41], cannot control MCMV infection in neurons. To relate our findings to cHCMV infection, we have developed a model of human fetal organotypic brain slice cultures that mimic the complexity of the human brain and maintain microglia [24]. We used this system to demonstrate that IFN- $\gamma$  treatment protected human neurons from HCMV infection. Thus, IFN- $\gamma$  can protect both human and mouse neurons from CMV infection.

The state of latency is defined as the presence of viral genomes without the production of new infectious virions [29]. While the viral gene expression is generally silenced during latency, it is suggested that stochastic transcription of CMV genes occurs during latency [76, 77]. Herpesviruses can replicate and establish latency in many cell types [78]. HCMV establishes latency in hematopoietic stem cells, myeloid progenitors, and monocytes, while monocytes, endothelial cells, and fibroblasts were shown to be sites of MCMV latency [23, 79]. Importantly, a limited number of studies have reported that HCMV genomes can be detected in more than 10% of adult brains, which is higher than expected based on the prevalence of cHCMV infection [2, 80]. The data presented in this study indicate that neurons are the main site of MCMV latency in the mouse brain, a state from which MCMV can reactivate upon loss of CD4<sup>+</sup> T-cells. HCMV can infect neurons and neural stem and precursor cells [53]. Interestingly, some studies suggest that primitive neural stem cells are infected nonproductively, with HCMV reactivating upon complete neuronal differentiation *ex vivo* [81], thus supporting our notion of the ability of CMV to reactivate in neurons. The exact mechanism of CD4<sup>+</sup> T-cell mediated prevention of MCMV reactivation remains unknown. We have previously shown that CD4<sup>+</sup> T-cells play a crucial role in establishing CD8<sup>+</sup> T-cell tissue residency in latently infected brains by promoting CD103 expression [30]. Thus, CD4<sup>+</sup> T-cells could also be critical for CD8<sup>+</sup> T cell-mediated surveillance of brain infection. Unlike professional antigen-presenting cells, neurons lack major histocompatibility complex (MHC

II) molecules, preventing them from directly triggering CD4<sup>+</sup> T-cells in an antigen-specific manner [82]. Thus, CD4<sup>+</sup> T-cells might control CMV reactivation in neurons through intermediate cells, such as MHC II expressing microglia, which can cross-present antigens to T-cells [57]. It was shown that uninfected microglia can effectively cross-present vesicular stomatitis virus (VSV) antigens acquired from neighboring neurons to CD8<sup>+</sup> T-cells to secure control of VSV in neurons [83], and it is plausible that such a mechanism might contribute to MCMV control. Finally, a TCR-independent mechanism of direct interaction between CD4<sup>+</sup> T-cells and neurons could be involved [84].

While animal models offer valuable insights, they also have limitations. CMV and its mammalian hosts have co-evolved, leading to unique viral genes and a strict host-species specificity, but also to some differences in pathogenesis [3]. However, the lack of non-invasive techniques for studying HCMV pathogenesis in the developing human brain presents a significant challenge, necessitating reliance on animal models. Therefore, we have utilized a well-established mouse model that recapitulates many aspects of human congenital CMV infection pathophysiology. Our findings demonstrate that MCMV infection in neonatal mice closely mirrors HCMV infection in humans, as both viruses have equal cell tropism and preference for infecting the hippocampus. Despite limited evidence suggesting the presence of HCMV in the brains of healthy adults, further investigations are necessary to validate our findings on potential HCMV latency in human neurons. Post-mortem analysis of the brains of individuals with a history of congenital HCMV infection could provide crucial insights into the mechanisms of HCMV latency in the human brain.

HCMV remains a major clinical problem, as there is no approved vaccine against HCMV, and pharmacotherapy during pregnancy is constrained by drug toxicity and teratogenicity [85]. HCMV is also linked to declines in neurocognitive and neuropsychiatric health and can be found in patients with glioblastoma multiforme [86, 87]. Therefore, a better understanding of the immune response to CMV infection in neuronal tissue remains a pressing need. This study provides novel insights into the virus-host interactions involved in controlling CMV infection in the brain and suggests that exploiting CD4<sup>+</sup> T-cell responses in preventive and therapeutic strategies might be beneficial in thwarting CMV-associated neurological complications.

#### Abbreviations

aCSF	artificial cerebrospinal fluid
cHCMV	congenital HCMV
CNS	Central nervous system
dpi	days post infection
HCMV	Human cytomegalovirus
hfOBSCs	Human fetal organotypic brain slice cultures

HIV	Human immunodeficiency virus
HSV	Herpes simplex virus
i.g	intra-gastric
i.p	intra-peritoneal
IFN- $\gamma$	interferon-gamma
IL-12	Interleukin-12
MCMV	Mouse CMV
MHC	Major histocompatibility complex
MIIEP	Major immediate-early promoter
MOI	Multiplicity of infection
SNHL	Sensorineural hearing loss
SSMs	Subcapsular sinus macrophages
Th1	T helper 1
T <sub>RM</sub> cells	Tissue-resident memory T-cells
WT	Wilde-type

## Supplementary Information

The online version contains supplementary material available at <https://doi.org/10.1186/s12974-025-03422-6>.

Supplementary Material 1

## Acknowledgements

We thank Mijo Golemac, Dijana Rumora, Leonarda Mikša, Ante Miše, Hana Mašinović, Cristina Paulović, and Antonija Šarlija for the excellent technical and administrative support. We thank Vanda Juranić Lisnić and Berislav Lisnić for the critical reading of the manuscript. Schematic representations are created with BioRender.com.

## Author contributions

Conceptualization: IB, FK. Resources: MGMGV, ZR, LČŠ, KMS. Investigation: FK, AM, ASR. Funding acquisition: IB, SJ, LČŠ, KMS, MGMGV. Writing—original draft: IB, FK. Writing—review & editing: IB, SJ, MGMGV.

## Funding

This work has been fully supported by "Research Cooperability" program of the Croatian Science Foundation funded by the European Union from the European Social Fund under the "Operational Programme Efficient Human Resources 2014–2020" (PZS-2019-02-7879, I.B.), the grant "Strengthening the capacity of CerVirVac for research in virus immunology and vaccinology" (KK.01.1.1.01.0006) granted to the Scientific Centre of Excellence for Virus Immunology and Vaccines and co-financed by the European Regional Development Fund (S.J.), the Croatian Science Foundation under the project numbers IP-2022-10-3371 and DOK-2020-01-5362 to (I.B.), and University of Rijeka (uniri-iskusni-biomed-23-231, I.B.), the German Scientific Foundation (DFG) through the grants EXC 2155 "RESIST"—Project ID 39087428 and FOR2830 (project 5) to LCS, the European Union's Horizon 2020 research and innovation program under Grant Agreement 793858 (to K.M.S.). The study was in part supported by The Lundbeck Foundation (R359-2020-2287) (author MGMGV).

## Data availability

No datasets were generated or analysed during the current study.

## Declarations

### Ethics approval and consent to participate

Human fetal brain tissue from legally terminated second trimester pregnancies (17–20 weeks) was obtained by the HIS-Mouse Facility of Academic Medical Center (AMC; Amsterdam, The Netherlands), after written informed consent of the mother for the tissue's use in research and with approval of the Medical Ethical Review Board of the AMC (MEC: 03/038) and Erasmus MC (MEC-2017-009). Study procedures were performed according to the Declaration of Helsinki, and in compliance with relevant Dutch laws and institutional guidelines.

### Consent for publication

Not applicable.

## Competing interests

The authors declare no competing interests.

Received: 31 December 2024 / Accepted: 18 March 2025

Published online: 29 March 2025

## References

1. Fowler K, Mucha J, Neumann M, Lewandowski W, Kaczanowska M, Grys M, et al. A systematic literature review of the global Seroprevalence of cytomegalovirus: possible implications for treatment, screening, and vaccine development. *BMC Public Health*. 2022;22(1):1659.
2. Manicklal S, Emery VC, Lazzarotto T, Boppana SB, Gupta RK. The silent global burden of congenital cytomegalovirus. *Clin Microbiol Rev*. 2013;26(1):86–102.
3. Reddehase M, Lemmermann N. Mouse model of cytomegalovirus disease and immunotherapy in the immunocompromised host: predictions for medical translation that survived the test of time. *Viruses*. 2018 Dec 6 [cited 2021 Mar 31];10(12):693.
4. Krstanović F, Britt WJ, Jonjić S, Brzić I. Cytomegalovirus infection and inflammation in developing brain. *Viruses*. 2021;13(6):1078.
5. Moulden J, Sung CYW, Brzić I, Jonjić S, Britt W. Murine models of central nervous system disease following congenital human cytomegalovirus infections. *Pathogens*. 2021;10(8).
6. Brzić I, Lisnić B, Krstanović F, Brune W, Hengel H, Jonjić S. Mouse models for cytomegalovirus infections in newborns and adults. *Curr Protoc*. 2022;2(9):1–23.
7. Kveštak D, Juranić Lisnić V, Lisnić B, Tomac J, Golemac M, Brzić I, et al. NK/ILC1 cells mediate neuroinflammation and brain pathology following congenital CMV infection. *J Exp Med*. 2021 May 3 [cited 2021 Mar 3];218(5).
8. Bantug GRB, Cekinovic D, Bradford R, Koontz T, Jonjić S, Britt WJ. CD8+ T Lymphocytes Control Murine Cytomegalovirus Replication in the Central Nervous System of Newborn Animals. *J Immunol*. 2008;181(3):2111–23.
9. Brzić I, Lisnić B, Brune W, Hengel H, Jonjić S. Cytomegalovirus infection: mouse model. *Curr Protoc Immunol*. 2018;122(1):e51.
10. Brzić I, Šušak B, Arapović M, Huszthy PC, Hiršl L, Kveštak D, et al. Brain-resident memory CD8+ T cells induced by congenital CMV infection prevent brain pathology and virus reactivation. *Eur J Immunol*. 2018;48(6):950–64.
11. Inoue S, Inoue M, Fujimura S, Nishinakamura R. A mouse line expressing Sall1-driven inducible Cre recombinase in the kidney mesenchyme. *Genesis*. 2010;48(3):207–12.
12. Kanda S, Tanigawa S, Ohmori T, Taguchi A, Kudo K, Suzuki Y, et al. Sall1 maintains nephron progenitors and nascent nephrons by acting as both an activator and a repressor. *J Am Soc Nephrol*. 2014;25(11):2584–95.
13. Jordan S, Krause J, Prager A, Mitrovic M, Jonjić S, Koszinowski UH, et al. Virus progeny of murine cytomegalovirus bacterial artificial chromosome pSM3fr show reduced growth in salivary glands due to a fixed mutation of MCK-2. *J Virol*. 2011;85(19):10346–53.
14. Tegtmeier P-K, Spanier J, Borst K, Becker J, Riedl A, Hirche C, et al. STING induces early IFN- $\beta$  in the liver and constrains myeloid cell-mediated dissemination of murine cytomegalovirus. *Nat Commun*. 2019;10(1):2830.
15. Pezoldt J, Wiechers C, Erhard F, Rand U, Bulat T, Beckstette M, et al. Single-cell transcriptional profiling of Splenic fibroblasts reveals subset-specific innate immune signatures in homeostasis and during viral infection. *Commun Biol*. 2021;4(1):1355.
16. Tischer BK, Smith GA, Osterrieder N. En passant mutagenesis: a two step markerless red recombination system. *Methods Mol Biol*. 2010;634:421–30.
17. Sampaio KL, Weyell A, Subramanian N, Wu Z, Sinzger C. A TB40/E-derived human cytomegalovirus genome with an intact US-gene region and a self-excisable BAC cassette for immunological research. *Biotechniques*. 2017;63(5):205–14.
18. Schindelin J, Arganda-Carreras I, Frise E, Kaynig V, Longair M, Pietzsch T, et al. Fiji: an open-source platform for biological-image analysis. *Nat Methods*. 2012;9(7):676–82.
19. Angelani CR, Carabias P, Cruz KM, Delfino JM, de Sautu M, Espelt MV, et al. A metabolic control analysis approach to introduce the study of systems in biochemistry: the glycolytic pathway in the red blood cell. *Biochem Mol Biol Educ*. 2018;46(5):502–15.
20. Pitulescu ME, Schmidt I, Benedetto R, Adams RH. Inducible gene targeting in the neonatal vasculature and analysis of retinal angiogenesis in mice. *Nat Protoc*. 2010;5(9):1518–34.

21. Bonavita CM, White TM, Francis J, Farrell HE, Davis-Poynter NJ, Cardin RD. The viral G-Protein-Coupled receptor homologs M33 and US28 promote cardiac dysfunction during murine cytomegalovirus infection. *Viruses*. 2023;15(3).
22. Simon CO, Seckert CK, Dreis D, Reddehase MJ, Grzimek NKA. Role for tumor necrosis factor alpha in murine cytomegalovirus transcriptional reactivation in latently infected lungs. *J Virol*. 2005;79(1):326–40.
23. Sitnik KM, Krstanović F, Gödecke N, Rand U, Kubsch T, Maaß H et al. Fibroblasts are a site of murine cytomegalovirus lytic replication and Stat1-dependent latent persistence in vivo. *Nat Commun*. 2023;14(1).
24. Rashidi AS, Tran DN, Peelen CR, van Gent M, Ouwendijk WJD, Verjans GMGM. Herpes simplex virus infection induces necroptosis of neurons and astrocytes in human fetal organotypic brain slice cultures. *J Neuroinflammation*. 2024;21(1):38.
25. Piccirilli G, Gabrielli L, Bonasoni MP, Chiereghin A, Turello G, Borgatti EC, et al. Fetal brain damage in human fetuses with congenital cytomegalovirus infection: histological features and viral tropism. *Cell Mol Neurobiol*. 2023;43(3):1385–99.
26. Koontz T, Bralic M, Tomac J, Pernjak-Pugel E, Bantug G, Jonjic S, et al. Altered development of the brain after focal herpesvirus infection of the central nervous system. *J Exp Med*. 2008;205(2):423–35.
27. Bernhardt R, Matus A. Light and electron microscopic studies of the distribution of microtubule-associated protein 2 in rat brain: a difference between dendritic and axonal cytoskeletons. *J Comp Neurol*. 1984;226(2):203–21.
28. Teissier N, Fallet-Bianco C, Delezoide AL, Laquerrière A, Marcorelles P, Khung-Savatovsky S, et al. Cytomegalovirus-induced brain malformations in fetuses. *J Neuropathol Exp Neurol*. 2014;73(2):143–58.
29. Reddehase MJ, Lemmermann NAW. Cellular reservoirs of latent cytomegaloviruses. *Med Microbiol Immunol*. 2019;208(3–4):391–403.
30. Brizic I, Hiršl L, Šuštić M, Golemac M, Britt WJ, Krmpotić A, et al. CD4 T cells are required for maintenance of CD8 TRM cells and virus control in the brain of MCMV-infected newborn mice. *Med Microbiol Immunol*. 2019;208(3–4):487–94.
31. Sacher T, Podlech J, Mohr CA, Jordan S, Ruzsics Z, Reddehase MJ, et al. The major virus-producing cell type during murine cytomegalovirus infection, the hepatocyte, is not the source of virus dissemination in the host. *Cell Host Microbe*. 2008;3(4):263–72.
32. Chappell-Maor L, Kolesnikov M, Kim J, Shemer A, Haimon Z, Grozovski J, et al. Comparative analysis of CreER Transgenic mice for the study of brain macrophages: A case study. *Eur J Immunol*. 2020;50(3):353–62.
33. Jonjić S, Mutter W, Weiland F, Reddehase MJ, Koszinowski UH. Site-restricted persistent cytomegalovirus infection after selective long-term depletion of CD4+T lymphocytes. *J Exp Med*. 1989;169(4):1199–212.
34. Swain SL, McKinstry KK, Strutt TM. Expanding roles for CD4+ T cells in immunity to viruses. *Nat Rev Immunol*. 2012;12(2):136–48.
35. Riera L, Gariglio M, Valente G, Müllbacher A, Museteanu C, Landolfo S, et al. Murine cytomegalovirus replication in salivary glands is controlled by both Perforin and granzymes during acute infection. *Eur J Immunol*. 2000;30(5):1350–5.
36. Lueder Y, Heller K, Ritter C, Keyser KA, Wagner K, Liu X, et al. Control of primary mouse cytomegalovirus infection in lung nodular inflammatory foci by Cooperation of interferon-gamma expressing CD4 and CD8 T cells. *PLoS Pathog*. 2018;14(8):e1007252.
37. Zangger N, Oderbolz J, Oxenius A. CD4 T Cell-Mediated immune control of cytomegalovirus infection in murine salivary glands. *Pathogens*. 2021;10(12):1531.
38. Trinchieri G. Interleukin-12 and the regulation of innate resistance and adaptive immunity. *Nat Rev Immunol*. 2003;3(2):133–46.
39. Hildreth AD, Padilla ET, Tafti RY, Legala AR, O'Sullivan TE. Sterile liver injury induces a protective tissue-resident cDC1-ILC1 circuit through cDC1-intrinsic cGAS-STING-dependent IL-12 production. *Cell Rep*. 2023;42(2):112141.
40. Krueger PD, Goldberg MF, Hong S-W, Osum KC, Langlois RA, Kotov DI, et al. Two sequential activation modules control the differentiation of protective T helper-1 (Th1) cells. *Immunity*. 2021;54(4):687–e7014.
41. Wu C, Wang X, Gadina M, O'Shea JJ, Presky DH, Magram J. IL-12 receptor beta 2 (IL-12R beta 2)-deficient mice are defective in IL-12-mediated signaling despite the presence of high affinity IL-12 binding sites. *J Immunol*. 2000;165(11):6221–8.
42. Kovalevich J, Langford D. Considerations for the use of SH-SY5Y neuroblastoma cells in neurobiology. *Methods Mol Biol*. 2013;1078:9–21.
43. Fernández-Alarcón C, Meyer LE, McVoy MA, Lokensgard JR, Hu S, Benneyworth MA, et al. Impairment in neurocognitive function following experimental neonatal Guinea pig cytomegalovirus infection. *Pediatr Res*. 2021;89(4):838–45.
44. Miller KD, Schnell MJ, Rall GF. Keeping it in check: chronic viral infection and antiviral immunity in the brain. *Nat Rev Neurosci*. 2016;17(12):766–76.
45. Figueiredo CP, Barros-Aragão FGQ, Neris RLS, Frost PS, Soares C, Souza INO, et al. Zika virus replicates in adult human brain tissue and impairs synapses and memory in mice. *Nat Commun*. 2019;10(1):3890.
46. Li Puma DD, Piacentini R, Leone L, Gironi K, Marcocci ME, De Chiara G, et al. Herpes simplex virus Type-1 infection impairs adult hippocampal neurogenesis via Amyloid-β protein accumulation. *Stem Cells*. 2019;37(11):1467–80.
47. Yong SJ, Yong MH, Teoh SL, Soga T, Parhar I, Chew J, et al. The hippocampal vulnerability to herpes simplex virus type I infection: relevance to Alzheimer's disease and memory impairment. *Front Cell Neurosci*. 2021;15:695738.
48. Zerboni L, Arvin A. Neuronal subtype and satellite cell tropism are determinants of Varicella-Zoster virus virulence in human dorsal root ganglia xenografts in vivo. *PLoS Pathog*. 2015;11(6):e1004989.
49. Cho H, Proll SC, Szretter KJ, Katze MG, Gale M, Diamond MS. Differential innate immune response programs in neuronal subtypes determine susceptibility to infection in the brain by positive-stranded RNA viruses. *Nat Med*. 2013;19(4):458–64.
50. Jehmlich U, Ritzer J, Grosche J, Härtig W, Liebert UG. Experimental measles encephalitis in Lewis rats: dissemination of infected neuronal cell subtypes. *J Neurovirol*. 2013;19(5):461–70.
51. Tan Y-L, Yuan Y, Tian L. Microglial regional heterogeneity and its role in the brain. *Mol Psychiatry*. 2020;25(2):351–67.
52. Davidson TL, Stevenson RJ. Vulnerability of the hippocampus to insults: links to Blood-Brain barrier dysfunction. *Int J Mol Sci*. 2024;25(4).
53. Cheeran MCJ, Lokensgard JR, Schleiss MR. Neuropathogenesis of congenital cytomegalovirus infection: disease mechanisms and prospects for intervention. *Clin Microbiol Rev*. 2009;22(1):99–126.
54. Potokar M, Zorec R, Jorgačevski J. Astrocytes are a key target for neurotropic viral infection. *Cells*. 2023;12(18):2307.
55. Farrell HE, Davis-Poynter N, Bruce K, Lawler C, Dolken L, Mach M, et al. Lymph node macrophages restrict murine cytomegalovirus dissemination. *J Virol*. 2015;89(14):7147–58.
56. Li Q, Barres BA. Microglia and macrophages in brain homeostasis and disease. *Nat Rev Immunol*. 2018;18(4):225–42.
57. Pavlou A, Mulenge F, Gern OL, Busker LM, Greimel E, Waltl I et al. Orchestration of antiviral responses within the infected central nervous system. *Cell Mol Immunol*. 2024.
58. Jonjić S, Pavić I, Lucin P, Rukavina D, Koszinowski UH. Efficacious control of cytomegalovirus infection after long-term depletion of CD8+T lymphocytes. *J Virol*. 1990;64(11):5457–64.
59. Gabrielli L, Bonasoni MP, Lazzarotto T, Lega S, Santini D, Foschini MP et al. Histological findings in fetuses congenitally infected by cytomegalovirus. *J Clin Virol*. 2009;46.
60. Sellier Y, Marliot F, Bessières B, Stirnemann J, Encha-Razavi F, Guilleminot T et al. Adaptive and innate immune cells in fetal human cytomegalovirus-infected brains. *Microorganisms*. 2020;8(2).
61. Soriano-Ramos M, Pedrero-Tomé R, Giménez Quiles E, Albert Vicent E, Baquero-Artigao F, Rodríguez-Molino P et al. T-Cell immune responses in newborns and Long-Term sequelae in congenital cytomegalovirus infection (CYTRIC Study). *J Pediatr*. 2024;114084.
62. Lidehäll AK, Engman M-L, Sund F, Malm G, Lewensohn-Fuchs I, Ewald U, et al. Cytomegalovirus-specific CD4 and CD8 T cell responses in infants and children. *Scand J Immunol*. 2013;77(2):135–43.
63. Tu W, Chen S, Sharp M, Dekker C, Manganello AM, Tongson EC, et al. Persistent and selective deficiency of CD4+T cell immunity to cytomegalovirus in immunocompetent young children. *J Immunol*. 2004;172(5):3260–7.
64. Bowen LN, Smith B, Reich D, Quezada M, Nath A. HIV-associated opportunistic CNS infections: pathophysiology, diagnosis and treatment. *Nat Rev Neurol*. 2016;12(11):662–74.
65. Nelson JA, Reynolds-Kohler C, Oldstone MB, Wiley CA. HIV and HCMV coinfect brain cells in patients with AIDS. *Virology*. 1988;165(1):286–90.
66. Bialas KM, Tanaka T, Tran D, Varner V, De La Rosa EC, Chiuppesi F, et al. Maternal CD4+T cells protect against severe congenital cytomegalovirus disease in a novel nonhuman primate model of placental cytomegalovirus transmission. *Proc Natl Acad Sci U S A*. 2015;112(44):13645–50.
67. Rollman TB, Berkebile ZW, Hicks DM, Hatfield JS, Chauhan P, Pravetoni M, et al. CD4+ but not CD8+T cells are required for protection against severe Guinea pig cytomegalovirus infections. *PLoS Pathog*. 2024;20(11):e1012515.

68. Griffin DE. Immune responses to RNA-virus infections of the CNS. *Nat Rev Immunol*. 2003;3(6):493–502.
69. Shrestha B, Wang T, Samuel MA, Whitby K, Craft J, Fikrig E, et al. Gamma interferon plays a crucial early antiviral role in protection against West Nile virus infection. *J Virol*. 2006;80(11):5338–48.
70. Patterson CE, Lawrence DMP, Echols LA, Rall GF. Immune-mediated protection from measles virus-induced central nervous system disease is noncytolytic and gamma interferon dependent. *J Virol*. 2002;76(9):4497–506.
71. Rodriguez M, Zocklein LJ, Howe CL, Pavelko KD, Gamez JD, Nakane S, et al. Gamma interferon is critical for neuronal viral clearance and protection in a susceptible mouse strain following early intracranial Theiler's murine encephalomyelitis virus infection. *J Virol*. 2003;77(22):12252–65.
72. Binder GK, Griffin DE. Interferon-gamma-mediated site-specific clearance of alphavirus from CNS neurons. *Science*. 2001;293(5528):303–6.
73. Parra B, Hinton DR, Marten NW, Bergmann CC, Lin MT, Yang CS, et al. IFN-gamma is required for viral clearance from central nervous system oligodendroglia. *J Immunol*. 1999;162(3):1641–7.
74. St. Leger AJ, Hendricks RL. CD8+T cells patrol HSV-1-infected trigeminal ganglia and prevent viral reactivation. *J Neurovirol*. 2011;17(6):528–34.
75. Frank GM, Lepisto AJ, Freeman ML, Sheridan BS, Cherpes TL, Hendricks RL. Early CD4(+) T cell help prevents partial CD8(+) T cell exhaustion and promotes maintenance of herpes simplex virus 1 latency. *J Immunol*. 2010;184(1):277–86.
76. Schwartz M, Stern-Ginossar N. The transcriptome of latent human cytomegalovirus. *J Virol*. 2019;93(11).
77. Griessl M, Renzaho A, Freitag K, Seckert CK, Reddehase MJ, Lemmermann NAW. Stochastic episodes of latent cytomegalovirus transcription drive CD8 T-Cell memory inflation and avoid immune evasion. *Front Immunol*. 2021;12.
78. Grinde B. Herpesviruses: latency and reactivation– viral strategies and host response. *J Oral Microbiol*. 2013;5(1):22766.
79. Cohen JI. Herpesvirus latency. *J Clin Invest*. 2020;130(7):3361–9.
80. Ribalta T, Martinez JA, Jares P, Muntané J, Miquel R, Claramonte X, et al. Presence of occult cytomegalovirus infection in the brain after orthotopic liver transplantation. *Virchows Arch*. 2002;440(2):166–71.
81. Belzile J-P, Stark TJ, Yeo GW, Spector DH. Human cytomegalovirus infection of human embryonic stem Cell-Derived primitive neural stem cells is restricted at several steps but leads to the persistence of viral DNA. *J Virol*. 2014;88(8):4021–39.
82. Liblau RS, Gonzalez-Dunia D, Wiendl H, Zipp F. Neurons as targets for T cells in the nervous system. *Trends Neurosci*. 2013;36(6):315–24.
83. Moseman EA, Blanchard AC, Nayak D, McGavern DB. T cell engagement of cross-presenting microglia protects the brain from a nasal virus infection. *Sci Immunol*. 2020;5(48):1–14.
84. Siffrin V, Radbruch H, Glumm R, Niesner R, Paterka M, Herz J, et al. In vivo imaging of partially reversible th17 cell-induced neuronal dysfunction in the course of encephalomyelitis. *Immunity*. 2010;33(3):424–36.
85. Leruez-Ville M, Foulon I, Pass R, Ville Y. Cytomegalovirus infection during pregnancy: state of the science. *Am J Obstet Gynecol*. 2020;223(3):330–49.
86. Cobbs CS, Harkins L, Samanta M, Gillespie GY, Bharara S, King PH, et al. Human cytomegalovirus infection and expression in human malignant glioma. *Cancer Res*. 2002;62(12):3347–50.
87. Gale SD, Farrer TJ, Erbstoesser R, MacLean S, Hedges DW. Human cytomegalovirus infection and neurocognitive and neuropsychiatric health. *Pathog (Basel Switzerland)*. 2024;13(5).

### Publisher's note

Springer Nature remains neutral with regard to jurisdictional claims in published maps and institutional affiliations.